Ontogeny of Mono- and Dikaryotic Rust Haustoria: Cytochemical and Ultrastructural Studies

J. Chong, D. E. Harder, and R. Rohringer

Agriculture Canada, Research Station, 195 Dafoe Road, Winnipeg, Manitoba R3T 2M9.

Based on a thesis submitted by the senior author for partial fulfillment of the requirements for a Ph.D. degree. Technical assistance of Ken Shewchuk is gratefully acknowledged. Contribution 957 from Agriculture Canada, Research Station, Winnipeg, Manitoba.

In rust-infected plant tissue, the haustoria produced by monodikaryotic or dikaryotic infections differ structurally in a number of ways. In general, the haustorial apparatus of dikaryotic infections appears to be highly specialized, with a well-defined haustorial mother cell (HMC) with modified walls at the penetration site, a narrow neck with a neck ring, a generally rounded body, and (in some cases) host cytoplasmic modifications at the host-haustorium interface. On the other hand, monokaryotic haustoria more closely resemble intercellular hyphae, and there is controversy whether they in fact should be designated as haustoria or as intracellular hyphae. What is known of the structural features of dikaryotic and monokaryotic haustoria and problems of terminology is described in detail by Littlefield and Heath (17) who designated them as D- and M-haustoria, respectively; their terminology will be retained in this paper.

Although the D- and M-haustoria of a number of rust fungi have been quite well characterized structurally, less is known of the cytological details of their formation. Only one report dealing with D-haustoria of *Uromyces phaseoli* f. sp. *vignae* (13) has described modifications in the form of long membrane protrusions at the septum separating the HMC from the intercellular hypha (the HMC septum). These membrane protrusions appear to have a specialized function, possibly similar to that postulated for the wall-membrane apparatus found in transfer cells of higher plants (8,13), but it is not known whether they also occur during the formation of M-haustoria. Relatively little is known about the chemical composition of the component parts of the D-haustorial apparatus, and how it may compare to that of M-haustoria.

We have studied in detail the structural aspects of the development of both D- and M-haustoria of *Puccinia coronata* Cda. f. sp. *avenae* Eriks. and (to a lesser extent) the D-haustoria of *Puccinia graminis* Pers. f. sp. *tritici* Eriks. and Henn. Various histochemical methods were used to obtain information on the chemical nature of haustorial walls and of associated structures. The significance of these results is discussed in connection with the probable mode of formation of D- and M-haustoria.

MATERIALS AND METHODS

Urediospore-derived infections. *Plant material and inoculation.* Seedlings of *Avena sativa* L. 'Pendek' and *Triticum aestivum* L. 'Chinese Spring' were grown and inoculated with a compatible race of *P. coronata* f. sp. *avenae* or *P. graminis* f. sp. *tritici*, respectively, as outlined previously (4,21).

Conventional fixing and staining for electron microscopy. Developing pustules were sampled at various times beginning 5 days after inoculation. The excised infected tissue was fixed with glutaraldehyde, then either postfixed with osmium tetroxide (OsO_4) or processed further without OsO_4 postfixation (4). Ultrathin sections were cut from near the edge and the center of rust colonies, mounted on formvar and carbon-coated 149-μm (100-mesh) or single-hole copper grids, and stained with uranyl acetate and lead concentrate.

Histochemical detection of polysaccharides. The periodic acid/chromic acid/phosphotungstic acid (PACP) (20) and periodic acid/thiocarbohydrazide/silver proteinate (PA-TCH-SP) (25) staining methods were used. Periodate oxidation (19) and control treatments for the PA-TCH-SP method (5,6) have been described (4).

For the study of lectin receptor sites, gold granules with an average diameter of 5 nm were prepared and coated with either Concanavalin A (Con A) or wheat germ lectin according to the techniques of Horisberger and Rosset (15). Infected tissue was fixed with glutaraldehyde as described above and embedded either in Spurr's embedding medium or Epon-Araldite. Ultrathin sections were floated for 2 hr on solutions containing gold-bound lectin, washed overnight with the appropriate buffer (15), deposited on copper grids, and poststained with 1% uranyl acetate. Control treatments were performed by floating the ultrathin sections on solutions containing gold-bound Con A or gold-bound wheat germ lectin in the presence of methyl α-D-methylmannopyranoside or chitin hydrolysate, respectively.

The $K_3Fe(CN)_6$ fixation method was used to localize glycogen (3).

Solvent extractions and enzyme treatments. Infected tissue fixed with glutaraldehyde was subjected to organic solvent extraction (ether/ethanol, acetone, or chloroform/methanol) or enzyme treatment before postfixation with OsO_4 according to Hickey and Coffey (14). The enzymes were: protease (Sigma, type V, purified, 1–5 mg/ml in 0.05 M Tris-HCl buffer, pH 7.5), cellulase (Sigma, type 1, practical grade, 5 mg/ml in 0.05 M phosphate buffer, pH 5.5). Ultrathin sections of specimens treated with organic solvents or enzymes were poststained with uranyl acetate and lead citrate as described above.

Basidiospore-derived infections. Buckthorn (*Rhamnus cathartica* L.) leaves naturally infected in late spring with basidiospores from overwintering telia of *P. coronata* f. sp. *avenae* were collected and processed for electron microscopy as described previously (9).

RESULTS

Urediospore-derived infections (*P. coronata* f. sp. *avenae* and *P. graminis* f. sp. *tritici*). Characteristic changes at the HMC septum were observed in *P. coronata* f. sp. *avenae* and *P. graminis* f. sp. *tritici* during early stages of haustorium formation. Elaborate membrane protrusions containing an electron-dense matrix (which will be referred to here as the protrusion matrix) were seen, together with a marked aggregation of mitochondria, on the hyphal side of the HMC septum (Fig. 1). Serial sections showed that these membrane protrusions originated from the fungal plasma membrane at the HMC septum. They were long, flattened cisternae closed at the end distal to the HMC septum (Figs. 1 and 2). At high magnification, interconnections between these membrane structures were visible (*unpublished*). In *P. coronata* f. sp. *avenae*, the membrane protrusions extended to a length of 4.2 μm during the period of host wall penetration and decreased in length during the subsequent formation of the haustorial neck. The cluster of mitochondria on the hyphal side of the HMC septa dispersed coincidentally with haustorium formation. The "angular" appearance of the membrane protrusions at this stage (Fig. 3) suggests that their reduction in size was caused by a rapid loss of the protrusion matrix. Septal membrane protrusions of HMC associated with older haustoria were in the shape of small ridges.

Haustorium formation began with the development of a penetration peg from the nonvacuolated HMC (Fig. 4).

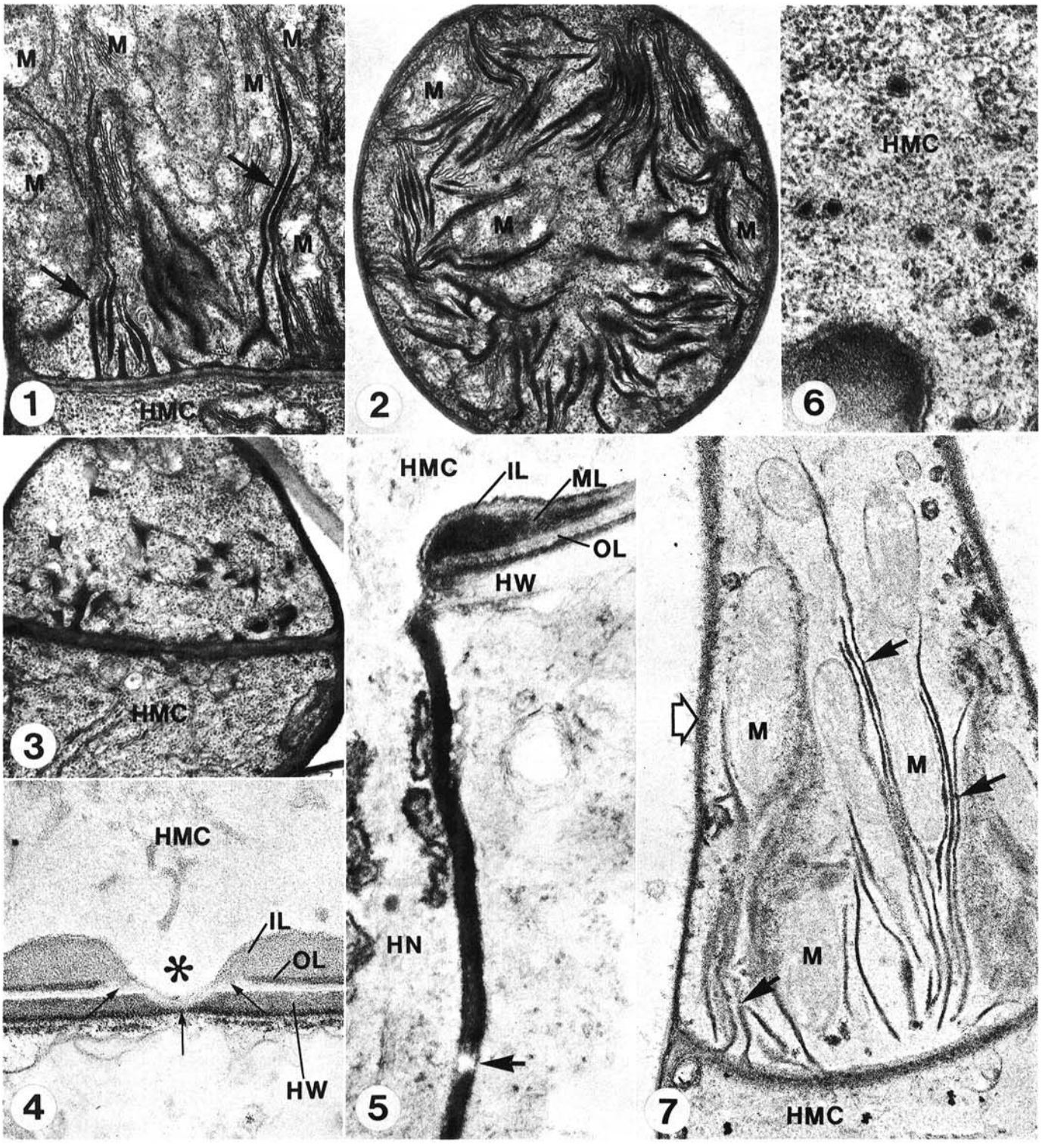

Figs. 1–7. Urediospore-derived infections. Fig. 5 is *Puccinia graminis* f. sp. *tritici* on wheat, others are *P. coronata* f. sp. *avenae* on oat. Abbreviations in figure labels and captions: Glt, glutaraldehyde; HMC, haustorial mother cell; HN, haustorial neck; IL, inner wall layer; M, mitochondria; ML, middle wall layer; OL, outer wall layer; PbC, lead citrate; PACP, periodic acid/chromate/phosphotungstate; PA-TCH-SP, periodic acid/thiocarbohydrazide/silver-proteinate; and UA, uranyl acetate. **1,** Longitudinal view of fungal plasma membrane protrusions (arrows) and associated mitochondria on the hyphal side of the HMC septum. Glt/OsO_4. UA/PbC. ×27,900. **2,** Cross-sectional view of membrane protrusions and associated mitochondria near the HMC septal region. Glt/OsO_4. UA/PbC. ×23,100. **3,** Membrane protrusions, decreased in size and angular in shape, after a young haustorium was formed. Glt/OsO_4. UA/PbC. ×23,100. **4,** Section from a series of closely adjacent sections to show a young penetration peg (asterisk), the wall of which appears to originate from the inner layer of the HMC wall (arrows). Glt/OsO_4. PA-TCH-SP. ×40,100. **5,** Three layers can be seen in the HMC wall at the site of penetration. Continuity is observed between the middle wall layer of HMC and haustorial neck wall. Neck ring (arrow) has been etched away by the PACP staining procedure. Glt/OsO_4. PACP. ×51,400. **6,** Membrane-bound densely stained granules in the HMC at the site of penetration. Glt/OsO_4. UA/PbC. × 66,100. **7,** Thiéry's staining of the protrusion matrix (arrows) and fungal walls (open arrow). Glt/OsO_4. PA-TCH-SP. ×31,100.

Penetration of the host wall appeared to be enzymatic since the host cell wall was never distorted at the site of penetration. In *P. coronata* f. sp. *avenae*, PA-TCH-SP treatment revealed that the thickened portion of the HMC wall at the site of penetration was composed of two layers: a thin, densely stained outer layer and a thick, lightly stained inner layer (Fig. 4). A thin wall layer that appeared to originate from the inner layer of the HMC wall was seen at the penetration region. In *P. graminis* f. sp. *tritici*, however, the HMC wall always contained three distinct layers at the site of penetration (Fig. 1 of reference 10). In the present study, the convex lens-shaped middle layer of the HMC wall was continuous with the neck wall (Fig. 5). In *P. coronata* f. sp. *avenae*, membrane-bound, electron-dense granules (Fig. 6), microtubules, and membranous materials (*unpublished*) were seen in the HMC cytoplasm at the penetration region and in young haustoria that had not yet formed a haustorial body. Only the microtubules were observed when a young haustorial body was present at the distal end of the neck. At this stage, when the haustorial body was about 3–4 μm in diameter, the haustorial neck did not have a neck ring structure (4,10).

In *P. coronata* f. sp. *avenae*, the neck ring was first observed as an electron-dense region in the neck wall (located about one third of the way down the neck from the haustorial body) when the haustorial body was about 5 μm in diameter. In mature haustoria, the neck ring was comprised of two cylindrical bands: a broad band designated α and a narrow band designated β (4). The β band was extractable with periodic acid, similar to the entire neck ring structures of *Melampsora lini* (16) and *P. graminis* f. sp. *tritici* (Fig. 5). In contrast, the α band was not affected by periodate treatment. With the use of energy-dispersive X-ray analysis (EDX), silicon was found to be the major element of the α band, and iron and phosphorus (possibly in the form of ferric pyrophosphate) were the major elements of the β band (4).

In unstained sections of glutaraldehyde/OsO_4-fixed specimens of *P. coronata* f. sp. *avenae*, both the protrusion matrix and the haustorial neck walls were osmiophilic. The protrusion matrix and the fungal walls were stained with PA-TCH-SP (Fig. 7). The HMC wall was composed of three distinct layers, all continuous with those of the HMC septum. The haustorial neck wall was composed of two layers: a thin, densely stained inner layer and a thick, lightly stained outer layer (Fig. 8). These two layers continued around the haustorial body to form the haustorial body wall.

In all controls for the PA-TCH-SP treatment, mycelial walls remained unstained. The silver staining of these walls observed after PA-TCH-SP treatment therefore was due to the presence of a polysaccharide containing vicinal hydroxyl groups (25). However, the protrusion matrix (Fig. 9) and haustorial walls (Fig. 10) stained intensely in a control treatment in which periodate oxidation had been omitted (the thiocarbohydrazide/ silver-proteinate control, TCH-SP). This property was shared with chloroplast plastoglobuli structures, thylakoid membranes, and other osmiophilic membrane structures, all known to contain lipid. After treatment with lipid solvents osmiophilia was absent in all of these structures and very little TCH-SP type of silver staining was observed in them or in the protrusion matrix and haustorial walls (not illustrated). Material remaining in the protrusion matrix and haustorial walls after extraction with lipid solvents (Figs. 11 and 12) reacted positively with the PA-TCH-SP stain, although staining intensity was much reduced. A similar pattern of Thiéry's staining was observed in glutaraldehyde-fixed specimens not treated with osmium tetroxide. This fixation procedure is known to extract all lipid components from samples during subsequent preparation steps (11). In fact, when thin sections of these specimens were subjected to the TCH-SP procedure, no silver staining was evident in the protrusion matrix (Fig. 13) and haustorial walls (Fig. 14), strengthening the conclusion that staining with this procedure is due to the presence of lipid.

De Bruijn's (3) fixation method was used to test for the presence of glycogen in fungal tissues. With this method, glycogen was detected in the form of electron dense granules in the hyphal cytoplasm in *P. coronata* f. sp. *avenae*. Both fungal walls and the protrusion matrix were electron lucent after this fixation.

Treatment of glutaraldehyde-fixed specimens with cellulase resulted in the removal of material from the host wall. It did not affect fungal walls or the protrusion matrix of *P. coronata* f. sp. *avenae*, indicating that cellulose is absent from these structures. With the colloidal gold method, there was heavy binding of Con A to fungal walls and to the protrusion matrix (Figs. 15 and 16). Gold-bound wheat germ lectin became bound to hyphal walls, but not to the protrusion matrix (Fig. 17) or young haustorial walls (Fig. 18). Binding of wheat germ lectin occurred on walls of bodies of mature haustoria, but never on neck walls regardless of the apparent age of the haustorium.

Treatment with proteolytic enzymes showed that protein was the major component of both the protrusion matrix (Fig. 19) and haustorial walls of *P. coronata* f. sp. *avenae* (Figs. 20 and 21) (4) but not of its hyphal walls. After protease treatment, a thin wall layer always remained around the haustorium. Staining with PA-TCH-SP treatment showed that this remaining layer contained polysaccharides with vicinal hydroxyl groups (Fig. 22). After protease treatment, all HMC observed were dislodged from the host cells and their haustoria (Figs. 20 and 21).

Diffuse electron-opaque material was often observed in the extrahaustorial matrix (EM) next to the haustorial wall of *P. coronata* f. sp. *avenae* (Fig. 23). The thickness of the EM and the amount of stained material appeared to increase with haustorium age, especially at the more distal end of the haustorial body. This was especially evident when serial sections of haustorial bodies were examined. The development of the EM was accompanied by a marked proliferation of tubules in the host cytoplasm. These were quite distinct from the host endoplasmic reticulum (Fig. 24). The membranes of these tubules were often seen connected to the invaginated host plasmalemma. By staining with PACP, we showed that the invaginated host plasmalemma at the distal portion of the haustorial body was more electron dense than the tubule membranes and other membrane structures in the host (Fig. 25). Both the EM and tubule contents reacted positively with Thiéry's stain (Fig. 26). Similar patterns of staining occurred in glutaraldehyde-fixed material not treated with osmium tetroxide, except that the EM stained more densely (Fig. 27). Cellulase treatment removed PA-TCH-SP-stainable material from the inside of tubules and from the EM, suggesting that these structures contain cellulose (Fig. 28). Solvent extraction did not seem to affect the amount of polysaccharide in the EM (*unpublished*). Protease treatment, however, removed almost all the EM material that was stainable with conventional stains (Fig. 29) and PA-TCH-SP treatment (Fig. 30).

Basidiospore-derived infections (*P. coronata* f. sp. *avenae*). The location of the last fungal septum outside the host cell appeared to vary with age of the M-haustorium. During early haustorium development, these septa were found at some distance from the penetration region. When the haustoria were more mature, the last septum outside the host cell occurred either close to or at the site of penetration, apparently due to new septum formation at this site. In older infections, the M-haustoria were septate (9). Septal regions of fungal cells near the site of host penetration were indistinguishable from each other and no structural changes comparable to those in D-infections were observed.

After PA-TCH-SP treatment, all fungal walls were intensely stained and were of similar thickness throughout the penetration region (Fig. 31). Relatively little constriction of the fungus was observed at the penetration site (Fig. 31). The M-haustoria of *P. coronata* f. sp. *avenae* did not possess a structure resembling the neck ring typical of D-haustoria and a clearly differentiated neck region was absent (Fig. 32).

The walls of M-haustoria were separated from the surrounding invaginated host plasmalemma. The intervening layer was designated as the extrahaustorial matrix (EM), analogous to that of the D-haustorial apparatus. The EM was very slight around most of the haustorial body, but was more pronounced at the distal portion of the haustorium (Fig. 32). After conventional staining (Fig. 33) or PA-TCH-SP treatment (Figs. 34 and 35) the EM was relatively electron opaque around the entire haustorial body. The fungal wall and the EM did not stain in control treatments, except when periodate oxidation was omitted (TCH-SP). After this

treatment, the EM along the proximal region of the haustorial body stained uniformly and was difficult to differentiate from the haustorial wall (Fig. 36). In the distal region, the EM stained less intensely than that in the proximal region and was clearly differentiated from the wall (Fig. 37). After PACP treatment, the EM in the distal region of the haustoria was strongly stained (Fig. 38). The EM in the proximal region, and the fungal wall, remained largely unstained. These results suggest that the EM in the distal region of haustoria has a different composition than the EM in the proximal region.

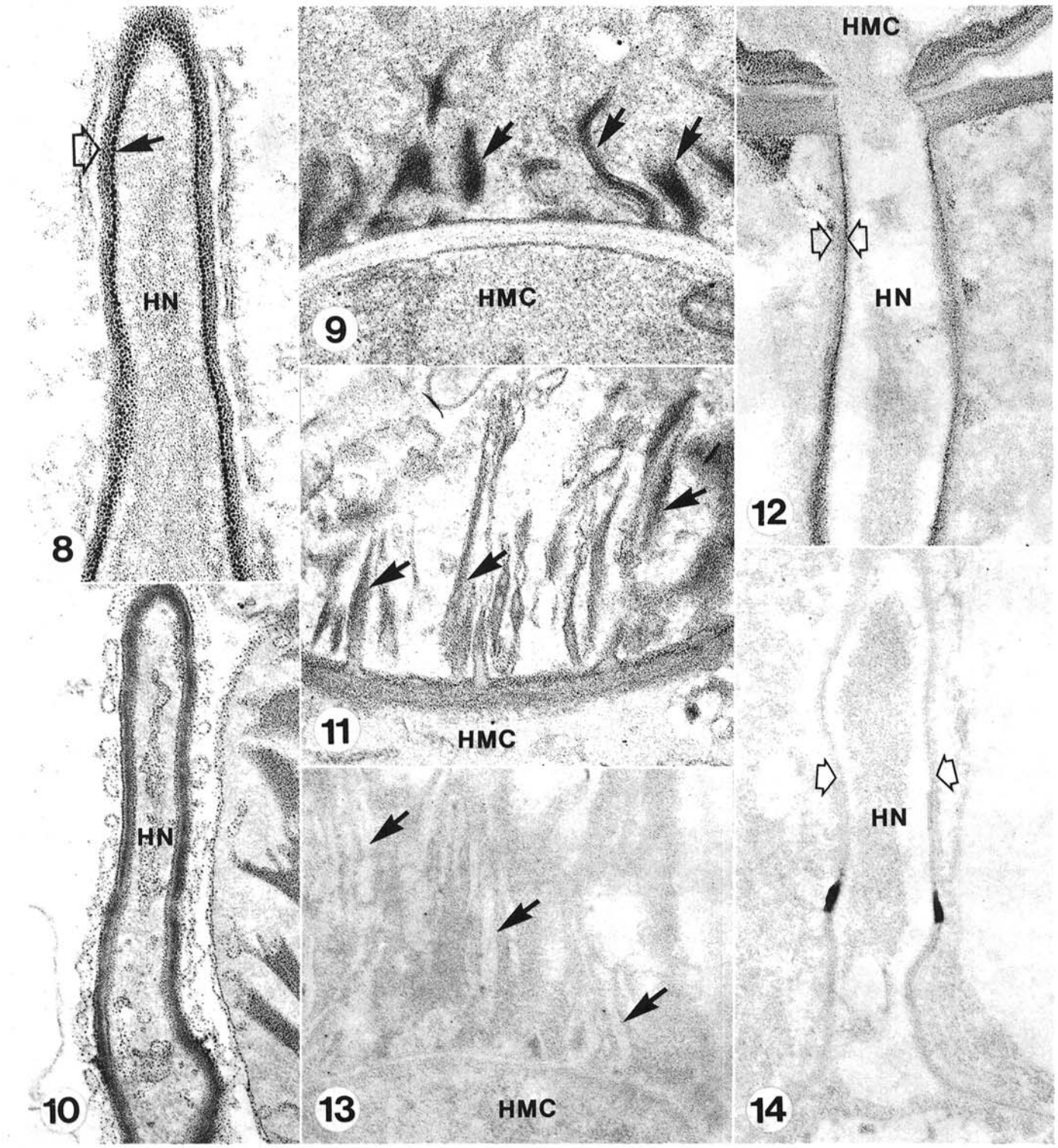

Figs. 8–14. Urediospore-derived infections of oat by *Puccinia coronata* f. sp. *avenae*. Abbreviations in figure labels and captions: Glt, glutaraldehyde; HN, haustorial neck; PA-TCH-SP, periodic acid/thiocarbohydrazide/silver-proteinate; and TCH-SP, thiocarbohydrazide/silver-proteinate control treatment. **8,** Thiéry's staining of haustorial neck wall showing a thin, densely stained inner layer (arrow) and a thick, lightly stained outer layer (open arrow). Glt/OsO_4. PA-TCH-SP. ×66,100. Figs. 9 and 10, Protrusion matrix (arrows) and haustorial neck wall, respectively, stained in control treatment. Glt/OsO_4. TCH-SP. **9,** ×50,000. **10,** ×34,000. **11,** Thiéry's staining of protrusion matrix (arrows) after lipid-solvent extraction. Staining intensity is reduced compared to that in Fig. 7. Glt/acetone/OsO_4. PA-TCH-SP. ×40,000. **12,** Thiéry's staining of haustorial neck wall (opposing arrows) after lipid-solvent extraction. Glt/chloroform-methanol/OsO_4. PA-TCH-SP. ×53,600. **13,** Protrusion matrix (arrows) not stained in control treatment. Glt. TCH-SP. ×42,900. **14,** Haustorial neck wall (arrows) not stained in control treatment. Glt. TCH-SP. ×30,000.

DISCUSSION

In the present study histochemical techniques provided some information about the chemical nature of structural components of the haustorial apparatus and the associated structures. In urediospore-derived infections it was shown by the PA-TCH-SP method that polysaccharides containing vicinal hydroxyl groups (25) were present in all fungal walls and in the protrusion matrix associated with the HMC septum. However, the intense staining of the protrusion matrix and of the haustorial wall should be

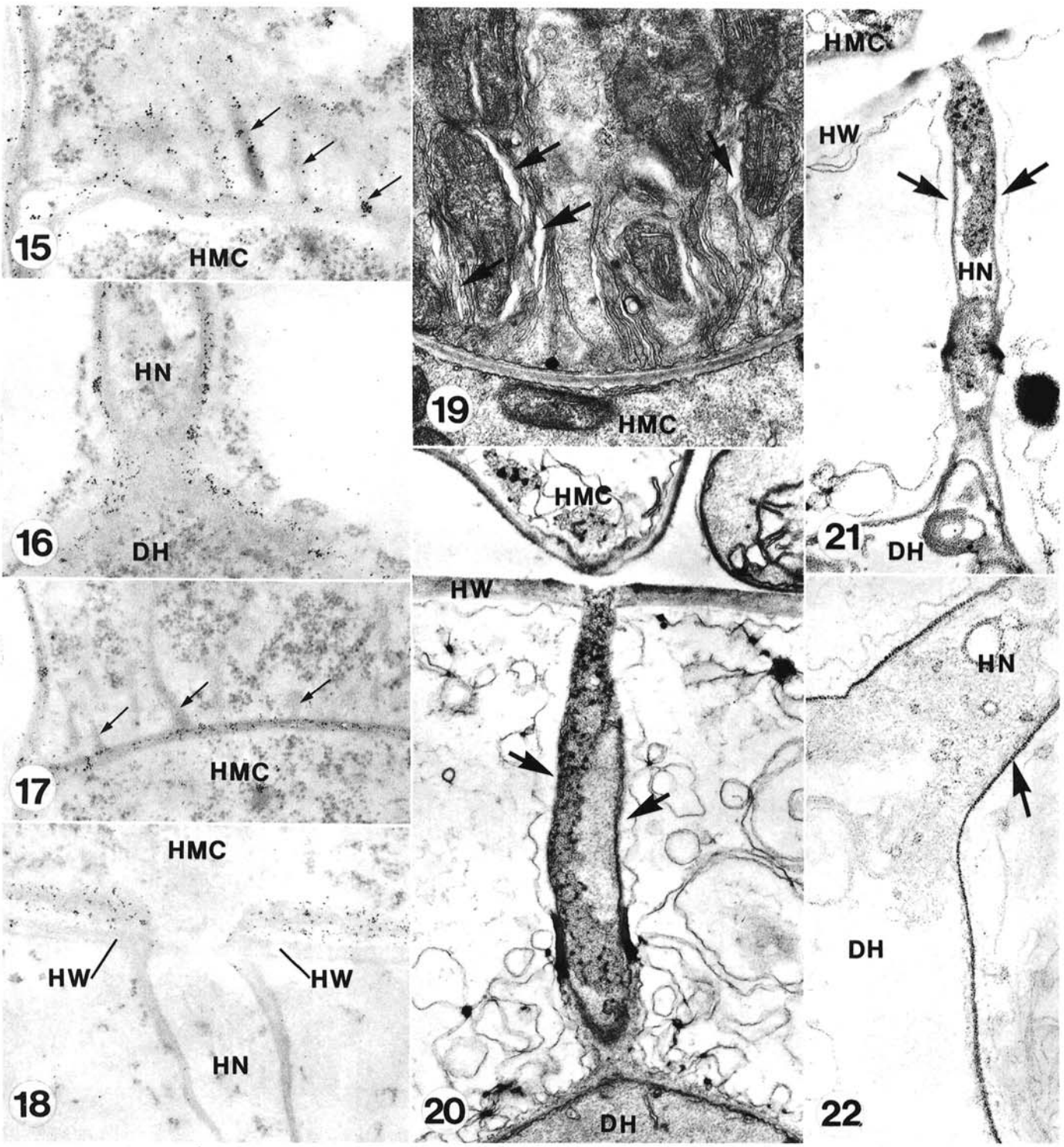

Figs. 15–22. Urediospore-derived infections. Fig. 18 is *Puccinia graminis* f. sp. *tritici* on wheat, others are *P. coronata* f. sp. *avenae* on oat. Abbreviations in figure labels and captions: Con A, concanavalin A; DH, D-haustorium; HMC, haustorial mother cell; HN, haustorial neck; HW, host cell wall; PA-TCH-SP, periodic acid/thiocarbohydrazide/silver-proteinate; PbC, lead citrate; TCH-SP, thiocarbohydrazide/silver-proteinate control treatment; UA, uranyl acetate; and WGL, wheat germ lectin. Figs. 15 and 16, Con A binding to fungal walls to **15,** the protrusion matrix (arrows) (×53,300) and **16,** haustorial walls (×44,400), respectively. Glt. Con A-gold. UA. Figs. 17 and 18, WGL binding to the fungal wall but not to **17,** the protrusion matrix (arrows) (×42,900) or **18,** the haustorial neck wall (×35,000). Glt. WGL-gold. UA. **19,** Protrusion matrix (arrows) electron lucent after protease treatment. Glt/protease/OsO_4. UA/PbC. ×29,800. **20,** Haustorial neck wall (arrows) electron lucent after protease treatment. Note separation of the HMC from its haustorium. Glt/protease/OsO_4. UA/PbC. ×26,300. **21,** Haustorial neck wall (arrows) unstained in TCH-SP control treatment after protease treatment. Note separation of HMC from its haustorium. Glt/protease/OsO_4. TCH-SP. ×20,600. **22,** Positive Thiéry's staining of the remaining thin wall layer (arrow) of haustorium after protease treatment. Glt/protease/OsO_4. PA-TCH-SP. ×42,900.

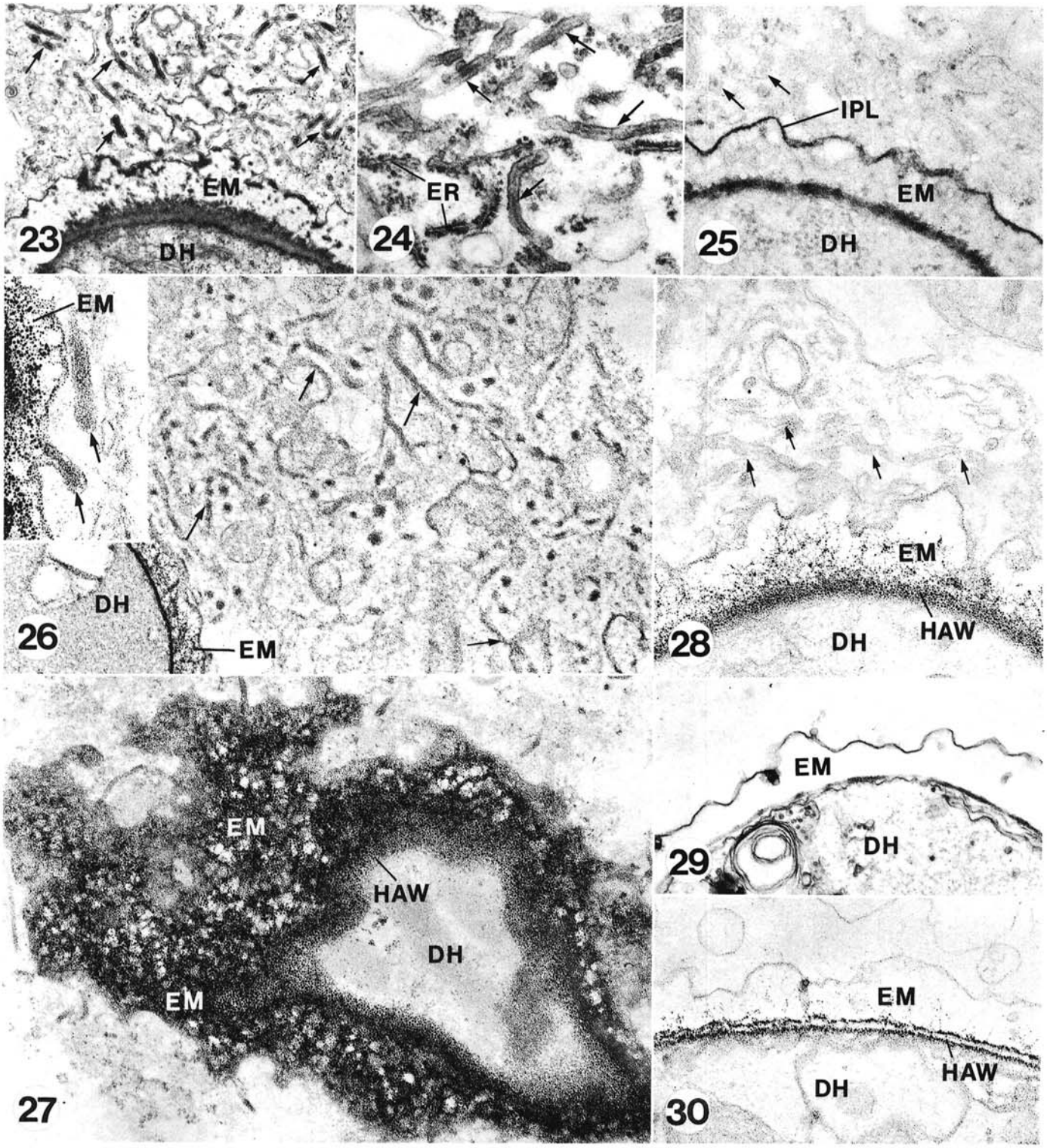

Figs. 23–30. Urediospore-derived infections of oat by *Puccinia coronata* f. sp. *avenae*. Abbreviations in figure labels and captions: DH, D-haustorium; EM, extrahaustorial matrix; ER, endoplasmic reticulum; HAW, haustorial wall; IPL, invaginated host plasmalemma; PACP, periodic acid/chromate/phosphotungstate; PA-TCH-SP, periodic acid/thiocarbohydrazide/silver-proteinate; PbC, lead citrate; and UA, uranyl acetate. **23,** Diffuse electron-opaque material in the EM. Note the presence of large tubules in the adjacent host cytoplasm (arrows). Glt/OsO_4. UA/PbC. ×17,100. **24,** Tubules contain electron-opaque material (arrows) and are distinct from the host endoplasmic reticulum. Glt/OsO_4. UA/PbC. ×43,800. **25,** Invaginated host plasmalemma stained more densely than tubule membranes (arrows) and other membranes of the host. Glt/OsO_4. PACP. ×38,600. **26,** Positive Thiéry's staining of contents of haustorium-associated tubules and the EM. ×39,300. Inset shows continuity of tubule with the EM. ×47,100. Glt/OsO_4. PA-TCH-SP. **27,** A near-tangential section through a haustorium at the distal region showing abundant stained material in the EM. Glt. PA-TCH-SP. ×30,000. **28,** Complete and partial removal of Thiéry's polysaccharide in the haustorium-associated host cytoplasmic tubules (arrows) and the EM, respectively, after cellulase treatment. Glt/cellulase/OsO_4. PA-TCH-SP. ×40,100. **29,** Absence of conventionally stainable materials in the EM after protease treatment. Glt/protease/OsO_4. UA/PbC. ×28,300. **30,** Remnants of Thiéry's stainable material in the EM after protease treatment. Glt/protease/OsO_4. PA-TCH-SP. ×35,700.

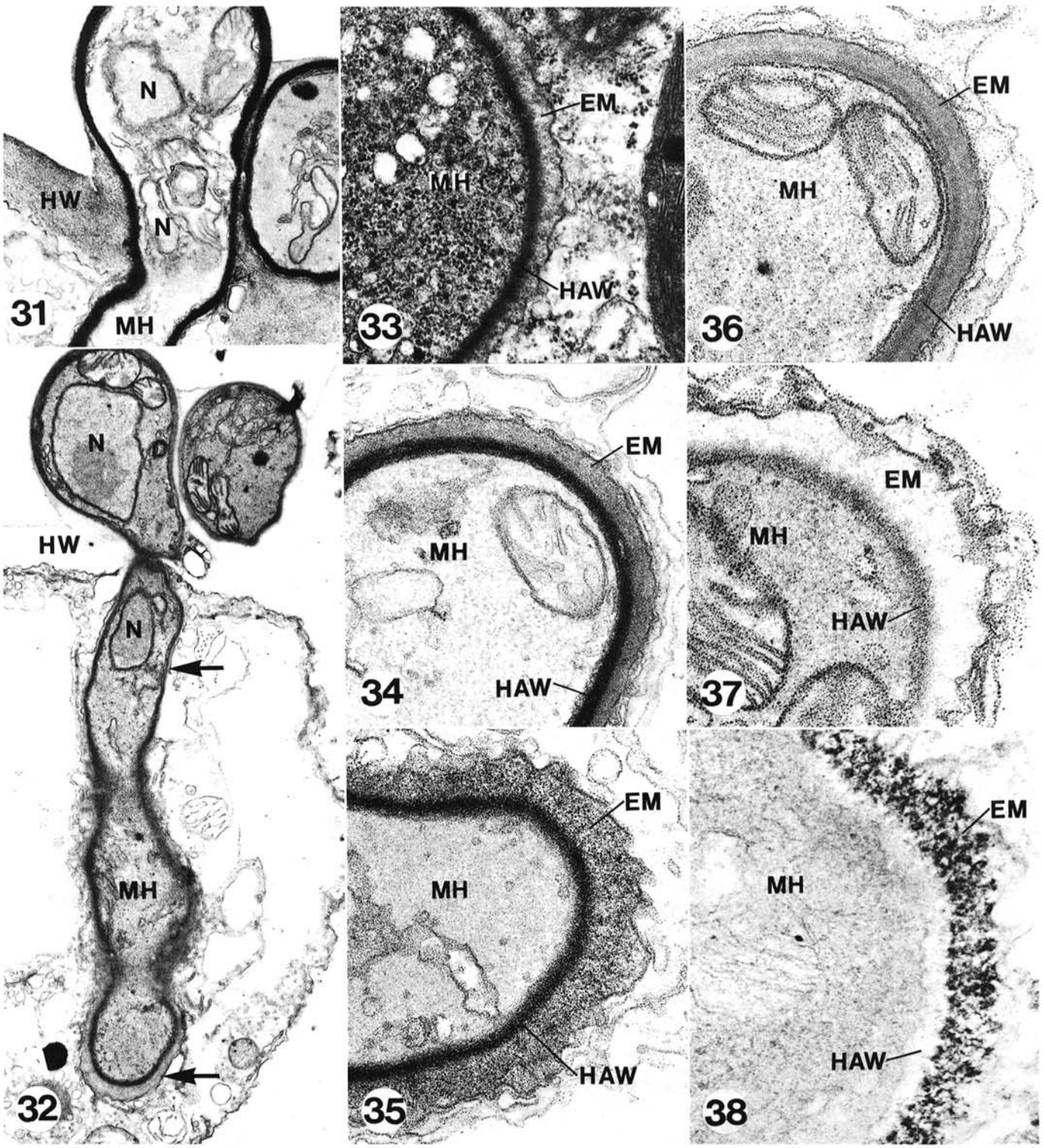

Figs. 31–38. Basidiospore-derived infections caused by *Puccinia coronata* f. sp. *avenae* in buckthorn leaves. Abbreviations in figure labels and captions: EM, extrahaustorial matrix; HAW, haustorial wall; HW, host cell wall; IPL, invaginated host plasmalemma; MH, M-haustoria; N, nucleus; PACP, periodic acid/chromate/phosphotungstate; PA-TCH-SP, periodic acid/thiocarbohydrazide/silver-proteinate; PbC, lead citrate; and UA, uranyl acetate. **31,** Fungal wall is intensely stained and is of similar thickness throughout the penetration region. Glt/OsO_4. PA-TCH-SP. ×18,200. **32,** An adjacent section to that in Fig. 31 showing the same M-haustorium. There is no clearly differentiated neck region in this M-haustorium and a neck ring is not present. Note the separation of the invaginated host plasmalemma (arrows) especially at the distal region of the M-haustorium to form an EM. Glt/OsO_4. TCH-SP. ×12,000. **33,** Electron-opaque material in the EM of a M-haustorium after conventional stains. Glt/OsO_4. UA/PbC. ×34,000. **34,** A cross section of a M-haustorium near the proximal region. The EM is relatively electron-opaque, but not as dense as the fungal cell wall. Glt/OsO_4. PA-TCH-SP. ×40,000. **35,** A section of a M-haustorium through the distal region, showing a densely stained EM. Glt/OsO_4. PA-TCH-SP. ×41,800. **36,** A closely adjacent section to that in Fig. 33. Both fungal wall and the EM are stained to the same extent in this control treatment. Glt/OsO_4. TCH-SP. ×40,000. **37,** A section of a M-haustorium through the distal region. The EM is more electron lucent than the fungal wall in this control treatment. Glt/OsO_4. TCH-SP. ×43,700. **38,** The EM of a M-haustorium along the distal region is intensely stained. Fungal wall and the invaginated host plasmalemma are largely unstained. Glt/OsO_4. PACP. ×77,100.

interpreted with caution, since both of these structures also stained after the control treatment in which periodate oxidation was omitted (TCH-SP). This staining behavior may be due to unsaturated lipids. These are known to be osmiophilic and the reduced osmium present after fixation will react with thiocarbohydrazide (12,18,24). Thiocarbohydrazide in turn will react with silver proteinate (22). The protrusion matrix and haustorial neck walls were in fact osmiophilic. The control treatment with TCH-SP caused silver staining not only in these structures but also in lipid droplets, chloroplast plastoglobuli, thylakoid membranes, and other membrane structures that were osmiophilic and known to contain lipids. After treatment of glutaraldehyde-fixed specimens with lipid solvents, the haustorial neck wall and the protrusion matrix were no longer osmiophilic and remained largely unstained after TCH-SP treatment, even after postfixation with OsO_4. They did, however, still react positively to PA-TCH-SP treatment, although staining intensity was much reduced compared to specimens not subjected to lipid extraction. This suggests that some of the polysaccharide in the protrusion matrix and neck wall were present in the form of lipopolysaccharide extractable with lipid solvents.

When gold-bound wheat germ lectin was used as a cytochemical marker (15), *N*-acetylglucosamine-containing receptors were demonstrated in walls of hyphae and in those of older haustorial bodies, but not in the protrusion matrix or the wall of the haustorial neck. Binding of the wheat germ lectin most likely indicates the presence of chitin, but this lectin will also bind to glycoproteins with available *N*-acetylglucosamine moieties. Gold-bound Con A became bound to the protrusion matrix and to all fungal walls. It is not known whether binding was due to glucan or mannan or both of them because Con A has an affinity for both (7). Further investigations are needed to determine which types of polysaccharide are present in these structures.

Treatment with protease indicated that protein is a major constituent of the protrusion matrix and haustorial walls, but not of other fungal walls. It is likely that protein is a main component of the substance by which the HMC adheres to the host wall, because all the HMC of *P. coronata* f. sp. *avenae* were found detached from the host cells and their haustoria after protease treatment. Moreover, our results indicate that polysaccharides with vicinal hydroxyl groups as well as lipids were largely removed from haustorial walls after protease treatment. It is possible that these polysaccharide and lipid components were present in the form of glycoprotein and lipoprotein.

The development of D-haustoria of *P. coronata* f. sp. *avenae* and *P. graminis* f. sp. *tritici* is similar to that of haustoria of *U. phaseoli* f. sp. *vignae* (13). The PA-TCH-SP procedure showed that a thin fungal wall was present around the penetration peg. In *P. graminis* f. sp. *tritici*, the lens-shaped middle layer of the HMC wall is continuous with the wall of the penetration peg and of the haustorial neck. This continuity was demonstrated by using the PACP method. It has also been shown in *M. lini* by using the same method (16). However, other histochemical tests on our material showed that the wall of the haustorial neck has a unique composition not found in other fungal walls. Evidently, the wall of the penetration peg marks the transition in chemical compostion between the wall of the HMC and that of the haustorial neck.

The characteristic membrane protrusions of the HMC septum that were observed in our study also have been noted in *U. phaseoli* f. sp. *vignae* (13), *P. hordei* (cited in reference 17) and possibly in *M. lini* (cited in reference 17). Association of the protrusions with a large number of mitochondria on the hyphal side of the HMC septum (reference 13 and present study) leads to speculation that materials are actively transported into the HMC during early haustorium differentiation. The membrane protrusions in *P. coronata* f. sp. *avenae* were long, flattened cisternae, closed at the end farthest from the HMC septum. In other material, membrane structures of similar shape have been regarded as functional sites where intensive secretion or absorption may take place (2,8). It is of interest that the matrix of septal protrusions and the haustorial neck wall reacted similarly chemically, indicating a similar composition. Since a marked reduction in size of the protrusions coincided with haustorial neck formation, it is possible that components of the membrane protrusions are used for the synthesis of the neck wall.

The extrahaustorial matrix (EM) (ie, the interface between the invaginated host plasmalemma and the haustorial wall) has long been a subject of debate. This is because the structural appearance of the EM can vary under different conditions of fixing and staining. For unknown reasons, the EM in specimens fixed with glutaraldehyde alone looked different and stained heavier after PA-TCH-SP treatment than those in specimens fixed with the conventional glutaraldehyde/OsO_4 process. The concept that the electron-lucent EM is an artifact of preparation (1) does not appear to hold, at least not in our studies with *P. coronata* f. sp. *avenae*. If the EM is real, it is of interest to determine its composition and origin. There is strong evidence that the composition of the EM of the D-haustorium of *P. coronata* f. sp. *avenae* differs from that of the wall of the haustorial body. The EM contains mainly polysaccharide and protein but no lipid or receptor sites for wheat germ lectin. It is probably free of chitin. The fact that the EM was almost completely electron lucent after protease treatment may indicate that polysaccharide was present mainly in the form of glycoprotein.

The development of the EM of D-haustoria of *P. coronata* f. sp. *avenae* was accompanied by a marked proliferation of tubules in the host cytoplasm. Both tubules and the EM lost electron-opaque material after cellulase treatment, indicating that cellulose may have been present in these structures before treatment with this enzyme preparation. Although the cellulase preparation was free from measurable proteolytic activity, it may have contained other polymer-degrading enzymes besides cellulase. With similar enzyme preparations, Scannerini and Bonfante-Fasolo (23) and Hickey and Coffey (14) reported cellulose to be a component of the EM in other plant-fungus interactions. Presence of cellulose in the EM of *P. coronata* f. sp. *avenae* suggests that the EM is not a fixation artifact and that at least this component is of host origin since it has not been detected anywhere else in the fungus. It is possible that deposition of cellulose in the EM is a response of the host that forms a cellulosic wall at this interface.

The M-haustoria of *P. coronata* f. sp. *avenae* had a much simpler structure than the D-haustoria. The last fungal septum located outside the host cell occurred at varying distances from the site of host penetration, and no structural differences could be observed between it and septa in other portions of the intercellular mycelium. Evidently, septation continued as though the M-haustorium is a normal growing hypha. Thus, the M-haustoria of *P. coronata* f. sp. *avenae* can be regarded as intercellular hyphae that have grown into the host cells. This conclusion is supported by the similar staining properties of the walls of the M-haustoria and those of other cells of the fungus. Doubtless, the designation of the M-haustoria as haustoria or as intracellular hyphae will remain controversial. However, the exiting of the M-haustoria of *P. coronata* f. sp. *avenae* from invaded cells has not been observed, as it has for several other rust fungi (see 17), indicating at least some specialization of the intracellular structures of *P. coronata* f. sp. *avenae*. Evidently, the M-haustoria of the rust fungi vary in degree of specialization, and it will be difficult to establish precise criteria by which to designate them.

LITERATURE CITED

1. Allen, F. H. E., Coffey, M. D., and Heath, M. C. 1979. Plasmolysis of rusted flax: a fine-structural study of the host-pathogen interface. Can. J. Bot. 57:1528-1533.
2. Berridge, M. J., and Oschman, J. L. 1972. Transporting Epithelia. Academic Press, New York. 95 pp.
3. Bruijn, W. C., De. 1973. Glycogen, its chemistry and morphologic appearance in the electron microscope. 1. A modified OsO_4 fixative which selectively contrasts glycogen. J. Ultrastruct. Res. 42:29-50.
4. Chong, J., and Harder, D. E. 1980. Ultrastructure of haustorium development in *Puccinia coronata avenae*. 1. Cytochemistry and electron-probe X-ray analysis of the haustorial neck ring. Can. J. Bot. (In press).
5. Courtoy, R., and Simar, L. J. 1974. Importance of controls for the

demonstration of carbohydrates in electron microscopy with the silver methenamine or the thiocarbohydrazide-silver proteinate methods. J. Microsc. 100:199-211.
6. Craig, A. S. 1974. Sodium borohydride as an aldehyde blocking reagent for electron microscope histochemistry. Histochemistry 42:141-144.
7. Goldstein, I. J., So, L. L., Yang, Y., and Callies, Q. C. 1969. Protein-carbohydrate interaction. XIX. The interaction of Concanavalin A with IgM and the glycoprotein phytohemagglutinins of the waxbean and the soybean. J. Immunol. 103:695-698.
8. Gunning, B. E. S. 1977. Transfer cells and their roles in transport of solutes in plants. Sci. Prog. 64:539-568.
9. Harder, D. E. 1978. Comparative ultrastructure of the haustoria in uredial and pycnial infections of *Puccinia coronata avenae*. Can. J. Bot. 56:214-224.
10. Harder, D. E., Rohringer, R., Samborski, D. J., Kim, W. K., and Chong, J. 1978. Electron microscopy of susceptible and resistant near-isogenic (*sr6*/*Sr6*) lines of wheat infected by *Puccinia graminis tritici*. 1. The host-pathogen interface in the compatible (*sr6*/*Sr6*) interaction. Can. J. Bot. 56:2955-2966.
11. Hayat, M. A. 1970. Principles and techniques of electron microscopy: biological applications. Vol. 1. Van Nostrand Reinhold Company. New York, Cincinnati, Toronto, London, and Melbourne. 412 pp.
12. Hayes, T. L., Lindgren, F. T., and Gofman, J. W. 1963. A quantitative determination of the osmium tetroxide-lipoprotein reaction. J. Cell. Biol. 19:251-255.
13. Heath, M. C., and Heath, I. B. 1975. Ultrastructural changes associated with the haustorial mother cell during haustorium formation in *Uromyces phaseoli* var. *vignae*. Protoplasma 84:297-314.
14. Hickey, E. L., and Coffey, M. D. 1978. A cytochemical investigation of the host-parasite interface in *Pisum sativum* infected by the downy mildew fungus *Peronospora pisi*. Protoplasma 97:201-220.
15. Horisberger, M., and Rosset, J. 1977. Colloidal gold, a useful marker for transmission and scanning electron microscopy. J. Histochem. Cytochem. 25:295-305.
16. Littlefield, L. J., and Bracker, C. E. 1972. Ultrastructural specialization at the host-pathogen interface in rust-infected flax. Protoplasma 74:271-305.
17. Littlefield, L. J., and Heath, M. C. 1979. Ultrastructure of rust fungi. Academic Press, New York, San Francisco, London. 277 pp.
18. Marinozzi, V. 1961. Silver impregnation of ultrathin sections for electron microscopy. J. Biophys. Biochem. Cytol. 9:121-211.
19. Nagahashi, G., Leonard, R. T., and Thomson, W. W. 1978. Purification of plasma membranes from roots of barley. Plant Physiol. 61:993-999.
20. Roland, J. C., Lembi, C. A., and Morre, D. J. 1972. Phosphotungstic acid-chromic acid as a selective electron-dense stain for plasma membranes of plant cells. Stain Technol. 47:195-200.
21. Samborski, D. J., Kim, W. K., Rohringer, R., Howes, N. K., and Baker, R. J. 1977. Histological studies on host-cell necrosis conditioned by the *Sr6* gene for resistance in wheat to stem rust. Can. J. Bot. 55:1445-1452.
22. Sannes, P. L., Spicer, S. S., and Katsuyama, T. 1979. Ultrastructural localization of sulphated complex carbohydrates with a modified iron diamine procedure. J. Histochem. Cytochem. 27:1108-1111.
23. Scannerini, S., and Bonfante-Fasolo, P. 1979. Ultrastructural cytochemical demonstration of polysaccharides and proteins within the host-arbuscule interfacial matrix in an endomycorrhiza. New Phytol. 83:87-94.
24. Seligman, A. M., Wasserkrug, H. L., and Hanker, J. S. 1966. A new procedure (OTO) for enhancing lipid-containing structures by bridging osmium to osmium-fixed tissue with thiocarbohydrazide (TCH). J. Cell. Biol. 30:424-432.
25. Thiéry, J.-P. 1967. Mise en évidence des polysaccharides sur coupes fines en microscopie électronique. J. Microsc. 6:987-1018.